Transthyretin Binding Heterogeneity and Anti-amyloidogenic Activity of Natural Polyphenols and Their Metabolites*

Paola Florio[‡1], **Claudia Folli**[§1], **Michele Cianci**[¶], **Daniele Del Rio**[§], **Giuseppe Zanotti**[‖], **and Rodolfo Berni**[‡2]

From the ‡Department of Life Sciences, University of Parma, 43124 Parma, Italy, the §Department of Food Science, University of Parma, 43124 Parma, Italy, the ¶European Molecular Biology Laboratory, 22607 Hamburg, Germany, and the ‖Department of Biomedical Sciences, University of Padua, 35131 Padua, Italy

Transthyretin (TTR) is an amyloidogenic protein, the amyloidogenic potential of which is enhanced by a number of specific point mutations. The ability to inhibit TTR fibrillogenesis is known for several classes of compounds, including natural polyphenols, which protect the native state of TTR by specifically interacting with its thyroxine binding sites. Comparative analyses of the interaction and of the ability to protect the TTR native state for polyphenols, both stilbenoids and flavonoids, and some of their main metabolites have been carried out. A main finding of this investigation was the highly preferential binding of resveratrol and thyroxine, both characterized by negative binding cooperativity, to distinct sites in TTR, consistent with the data of x-ray analysis of TTR in complex with both ligands. Although revealing the ability of the two thyroxine binding sites of TTR to discriminate between different ligands, this feature has allowed us to evaluate the interactions of polyphenols with both resveratrol and thyroxine preferential binding sites, by using resveratrol and radiolabeled T4 as probes. Among flavonoids, genistein and apigenin were able to effectively displace resveratrol from its preferential binding site, whereas genistein also showed the ability to interact, albeit weakly, with the preferential thyroxine binding site. Several glucuronidated polyphenol metabolites did not exhibit significant competition for resveratrol and thyroxine preferential binding sites and lacked the ability to stabilize TTR. However, resveratrol-3-O-sulfate was able to significantly protect the protein native state. A rationale for the *in vitro* properties found for polyphenol metabolites was provided by x-ray analysis of their complexes with TTR.

Amyloidoses are particularly relevant human diseases that are characterized by the extracellular deposition of normally soluble proteins. To date, more than 30 human precursor proteins have been associated with amyloidoses, in which amyloid deposits contain highly ordered cross-β-sheet fibrillar components. Human transthyretin (TTR)[3] represents a relevant amyloidogenic protein whose amyloidogenic potential is enhanced by a large number of specific point mutations. In fact, although WT TTR gives rise to a sporadic disease called senile systemic amyloidosis in the old age (1), genetic TTR variants are involved in the more aggressive hereditary TTR amyloidoses, in which peripheral nervous system (familial amyloidotic polyneuropathy) and heart (familial amyloidotic cardiomiopathy) are mainly affected (2, 3).

TTR is a homotetramer of ~55 kDa physiologically involved in the transport of thyroxine (T4) in extracellular fluids, both plasma and cerebrospinal fluid, and in the co-transport of vitamin A, by forming a macromolecular complex with RBP4 (retinol-binding protein 4), the specific plasma carrier of retinol (4, 5). In TTR, the four monomers are assembled according to a 222 symmetry to give rise to a dimer of dimers. Specifically, two monomers are connected to each other through a net of H-bond interactions involving the two edge β-strands H and F, to form a stable dimer, whereas two dimers associate back to back through a limited number of contacts. One of the 2-fold symmetry axes coincides with the long channel that transverses the entire tetramer and harbors two symmetrical binding sites for T4, at the dimer-dimer interface. Despite the presence in the TTR tetramer of very similar binding sites, which are both occupied in the crystal with roughly similar mode of binding by T4 (5), the binding of T4 in solution is characterized by a strong negative cooperativity, whose molecular basis remains elusive. Biochemical data revealed a 100-fold difference in the binding constants for the first and second T4 bound to TTR (6).

According to computational analysis human TTR possesses a relatively high intrinsic propensity to β-aggregation (7). Experimental evidence has been presented to indicate that such a propensity is enhanced in amyloidogenic genetic TTR variants as a result of a destabilization of the native TTR structure induced by amyloidogenic mutations (8–13). It should be pointed out that T4 and other specific TTR ligands establish interactions with the two subunits whose residues line along each hormone binding cavity in the central channel. As a result, the subunits forming each binding cavity become connected to

[1] These authors contributed equally to this work.
[2] To whom correspondence should be addressed: Dept. of Life Sciences, University of Parma, Parco Area delle Scienze 23/A, 43124 Parma, Italy. Tel.: 39-0521-905645; E-mail rodolfo.berni@unipr.it.

[3] The abbreviations used are: TTR, transthyretin; T4, thyroxine.

each other through several interactions mediated by the TTR ligand, which leads to a drastic stabilization of the native TTR tetramer (2, 14–16). A large number of potential TTR stabilizers have been tested for their ability to interact with the T4 binding sites in TTR and to stabilize its native structure (14). Among them, tafamidis and diflunisal were found to be effective in slowing neurological impairment in TTR amyloidosis (17, 18) and are now available for most patients (19).

Polyphenols represent a large family of natural compounds, widely distributed in the plant kingdom, which are characterized by the association of multiple phenolic groups to give different classes of biologically active compounds, such as flavonoids and stilbenoids. Polyphenols are the most abundant antioxidant compounds present in human diet, and potential beneficial activities in the prevention of degenerative diseases, including amyloidoses, have been attributed to these molecules (20, 21). Previous studies provided evidence for the specific interactions of resveratrol (22) and of some flavonoids (23–25) with the T4 binding sites of TTR and for their ability to stabilize TTR tetramer and to inhibit fibril formation (23–26). Moreover, data indicating the presence of distinct preferential binding sites in TTR for T4 and some polyphenols have recently been obtained (27). Despite the fact that polyphenols show promising features as potential disease-preventing agents, their bioavailability is low or very low (20), and because of their efficient metabolic degradation, their concentrations in plasma are markedly lower than those at which most of *in vitro* biological activities are reported. Glucuronidation and sulfate conjugation products of polyphenols are major metabolites found in plasma (20). To date very few studies have been carried out to establish the biological activities of these metabolic derivatives. We report here on a comparative analysis of the interactions of resveratrol, flavonoids (genistein, apigenin, daidzein), and some of their major metabolites with TTR and of their stabilizing effect on protein native structure and provide additional evidence for functional heterogeneity of TTR binding sites.

Experimental Procedures

Materials—L-Thyroxine (T4), genistein, apigenin, and *trans*-resveratrol, were from Sigma-Aldrich; resveratrol-3-*O*-sulfate, resveratrol-4′-*O*-glucuronide, and resveratrol-3-*O*-glucuronide were from Bertin Pharma; and genistein-7-*O*-glucuronide and daidzein-7-*O*-glucuronide were from Extrasynthese. Radiolabeled T4 (L-[^{125}I]T4; specific activity, ~1250 μCi/μg) was from PerkinElmer Life Sciences. All other chemicals were of analytical grade. Expression and purification of WT human TTR was performed as previously described (28).

Fluorometric Binding Assays—Fluorescence binding experiments were carried out in 50 mM sodium phosphate buffer, 150 mM sodium chloride, pH 7.4, at 25 °C, using a PerkinElmer Life Sciences LS-50B spectrofluorometer. The interactions between WT TTR and resveratrol and its derivatives were analyzed by monitoring the enhancement of their fluorescence intensity upon binding to TTR. Recombinant TTR was supplemented with resveratrol or resveratrol metabolites (dissolved in DMSO), and fluorescence emission spectra from 350 to 500 nm were recorded (excitation at 320 nm). The evaluation of the ability of T4 (dissolved in 10 mM sodium hydroxide) (6), res-

veratrol metabolites, and flavonoids (dissolved in DMSO) to compete with TTR-bound resveratrol was based on the changes in the fluorescence emission spectra of resveratrol. The displacement of TTR-bound resveratrol was monitored by the decrease of its fluorescence intensity (excitation and emission at 320 and 390 nm, respectively).

Competition Binding Assays in the Presence of Radiolabeled T4—The interactions between recombinant WT TTR and stilbenoids, flavonoids, and their derivatives were further investigated by competitive binding assays in the presence of radiolabeled T4. Recombinant WT TTR (3 μM) was incubated with a trace amount (~0.3 nM) of radiolabeled T4 or with 3 μM nonradiolabeled T4 in the presence of ~0.3 nM radiolabeled T4, in the absence or in the presence of increasing concentrations of polyphenols, in 50 mM sodium phosphate buffer, 150 mM sodium chloride, pH 7.4, for 1 h at room temperature. Samples were then subjected to nondenaturing PAGE, and radioactivity signals were recorded with a Cyclone storage phosphor screen (Packard BioScience). Competition binding assays in the presence of radiolabeled T4 were also conducted for TTR present in human plasma. Aliquots of plasma (10 μl) were incubated overnight with a trace amount (~1 nM) of radiolabeled T4 and increasing concentrations (from 1 to 100 μM) of polyphenols; the analysis of plasma samples was performed as described for recombinant TTR.

Stabilization of the TTR Tetramer against Urea Denaturation—Recombinant WT TTR (10 μM) in 10 mM sodium phosphate, 150 mM NaCl, pH 7.4, was supplemented with 2 molar equivalents of polyphenols (resveratrol, genistein, apigenin, and daidzein) or with 2 molar equivalents of polyphenol metabolites (resveratrol-3-*O*-sulfate, resveratrol-3-*O*-glucuronide, resveratrol-4′-*O*-glucuronide, genistein-7-*O*-glucuronide, and daidzein-7-*O*-glucuronide). After 1 h of incubation at room temperature, urea was added to the samples (final concentration, 5 M), and the mixtures were further incubated at 4 °C for 24 h. TTR was then cross-linked in the presence of 2.5% glutaraldehyde as described (29), and samples were finally subjected to SDS-PAGE. The intensity of the electrophoretic bands corresponding to TTR monomer was quantified by using a BIO-RAD GS-800 densitometer. The extent of protection of TTR in the presence of the denaturing agent was revealed by estimating the quantity of protein monomer of each sample compared with that present in the sample of TTR in the absence of ligands.

Inhibition of TTR Fibrillogenesis at Moderately Acidic pH—*In vitro* TTR fibrillogenesis at moderately acidic pH was monitored by following the increase in turbidity, estimated spectrophotometrically at 400 nm, as described previously (30). 7.2 μM WT TTR was preincubated with 3 molar equivalents of polyphenols or with DMSO or 3 molar equivalents of diflunisal as negative and positive controls, respectively, at neutral pH (10 mM sodium phosphate buffer, pH 7, 100 mM KCl, 1 mM EDTA) for 3 h at room temperature, prior to incubation at acidic pH upon addition of an equal volume of 100 mM sodium acetate, 100 mM KCl, 1 mM EDTA, pH 4.2 (final pH 4.3), at 37 °C to promote fibrillogenesis.

Crystallization and Structure Determination—Crystals of WT human TTR-ligand complexes were obtained at room

temperature in ~1 week by co-crystallization, using the hanging drop vapor diffusion method. The protein (5 mg/ml) in 20 mM sodium phosphate, pH 7, was incubated with a 4-fold molar excess of ligands solubilized in DMSO. In the case of the mixed complex TTR-resveratrol-T4, the three components were mixed in a 1:1:1 stoichiometry. Drops were formed by mixing equal volumes of the solution containing ligand-TTR complexes and of the reservoir/precipitant solution (≈2.2 M ammonium sulfate, 0.1 M KCl, 0.03 M sodium phosphate, pH 7.0). Diffraction data were collected at 100 K using synchrotron radiation at the European Molecular Biology Laboratory P13 Beamline at the Petra III storage ring (c/o DESY, Hamburg, Germany), with the exception of TTR in complex with resveratrol-3′-O-sulfate and of the mixed complex resveratrol-T4-TTR that were measured at the Synchrotron Light Source facility (Villigen, Switzerland). Crystallographic data were processed using the program XDS (31) and scaled with AIMLESS (32) while keeping the Friedel's pair separate. The structures of WT TTR-ligand complexes were refined starting from that of the dimer of WT human TTR as a template (Protein Data Bank code 1F41) (33). The models were subjected to rigid body minimization and subsequently to refinement steps with Phenix (34). Map visualization and manual adjustment of the models were performed using the Coot graphic interface (35). Atomic coordinates of the ligand molecules and restraints were obtained through the PRODRG server (36) or Elbow program within Phenix suite (34). The ligand orientation was determined by inspecting the electron density map, calculated with $|F_{\mathrm{obs}} - F_{\mathrm{calc}}|$ coefficients, and calculated with phases from the model, deprived of the ligand.

Results

Comparative Analysis of the Interactions of Polyphenols with TTR Using Resveratrol and Radiolabeled T4 as Probes—The structural formulae of the compounds investigated in this study are shown in Fig. 1.

Competition between Resveratrol, Resveratrol Metabolites, and T4—The fluorescence emission of uncomplexed resveratrol in solution is quite low and increases substantially upon binding to TTR (Fig. 2a). Thus, the binding of resveratrol to TTR, as well as its displacement by competitors, can be conveniently monitored by following changes in the fluorescence emission of this compound (16). Interestingly, the increase in the fluorescence signal associated with resveratrol binding under our experimental conditions (in which protein and ligand concentrations are in the micromolar range) is nearly complete upon addition of one equivalent of ligand to TTR, and only a slight increase in the fluorescence emission of resveratrol is achieved by increasing substantially ligand concentration (Fig. 2a). This result is consistent with different binding affinities of resveratrol for the two sites on TTR, in keeping with the negative cooperativity for the binding of T4 to TTR (6). The ability of competitors to displace TTR-bound resveratrol from its high affinity binding site was then evaluated. To facilitate the interpretation of the results of competitive binding assays for a protein that possesses two binding sites with remarkably different binding affinities, such assays were carried out in the presence of one equivalent of resveratrol bound per TTR tetramer.
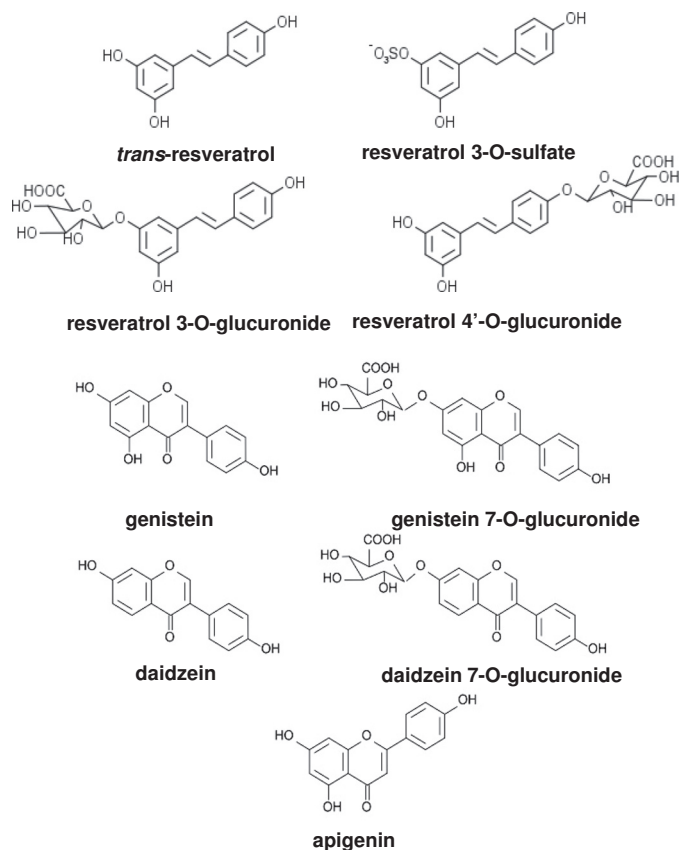

FIGURE 1. **Structural formulae of stilbenoids and flavonoids investigated in this study.**

The second probe used to reveal the binding of polyphenols to TTR in competition binding assays was radiolabeled T4, which interacts strongly with one of the two binding sites of TTR because of the above mentioned negative cooperativity.

Because of the lack of fluorescence of T4 in the emission region of resveratrol, the binding of the natural ligand to TTR could be revealed by the displacement of TTR-bound resveratrol. Quite unexpectedly, however, 1–6 molar equivalents of T4 did not effectively compete with bound resveratrol, because its fluorescence intensity was only slightly affected in the presence of T4 (Fig. 2b), in agreement with previous binding data for both WT TTR and I84S TTR (16). However, upon addition of T4, an appreciable red shift (by ~5 nm) for the emission maximum of resveratrol fluorescence was observed, clearly indicating an interaction of T4 with TTR, likely occurring at the second site present in TTR, distinct from that occupied by resveratrol, and the presence of functional binding site heterogeneity in the TTR molecule. The same result was obtained when the addition of resveratrol was preceded by that of T4 (Fig. 2b). The observed red shift induced by T4 binding suggests the existence of a communication between the two binding sites in TTR. To confirm the existence of TTR binding site heterogeneity, presumably induced by the interaction with one of the two ligands, at variance with the internal symmetry of the two binding sites in uncomplexed TTR (33), an experiment has been carried out in which TTR preincubated with a trace amount of radiolabeled T4 increasing quantities (up to 100 μM) of resveratrol or some of its main metabolites (resveratrol-3-O-
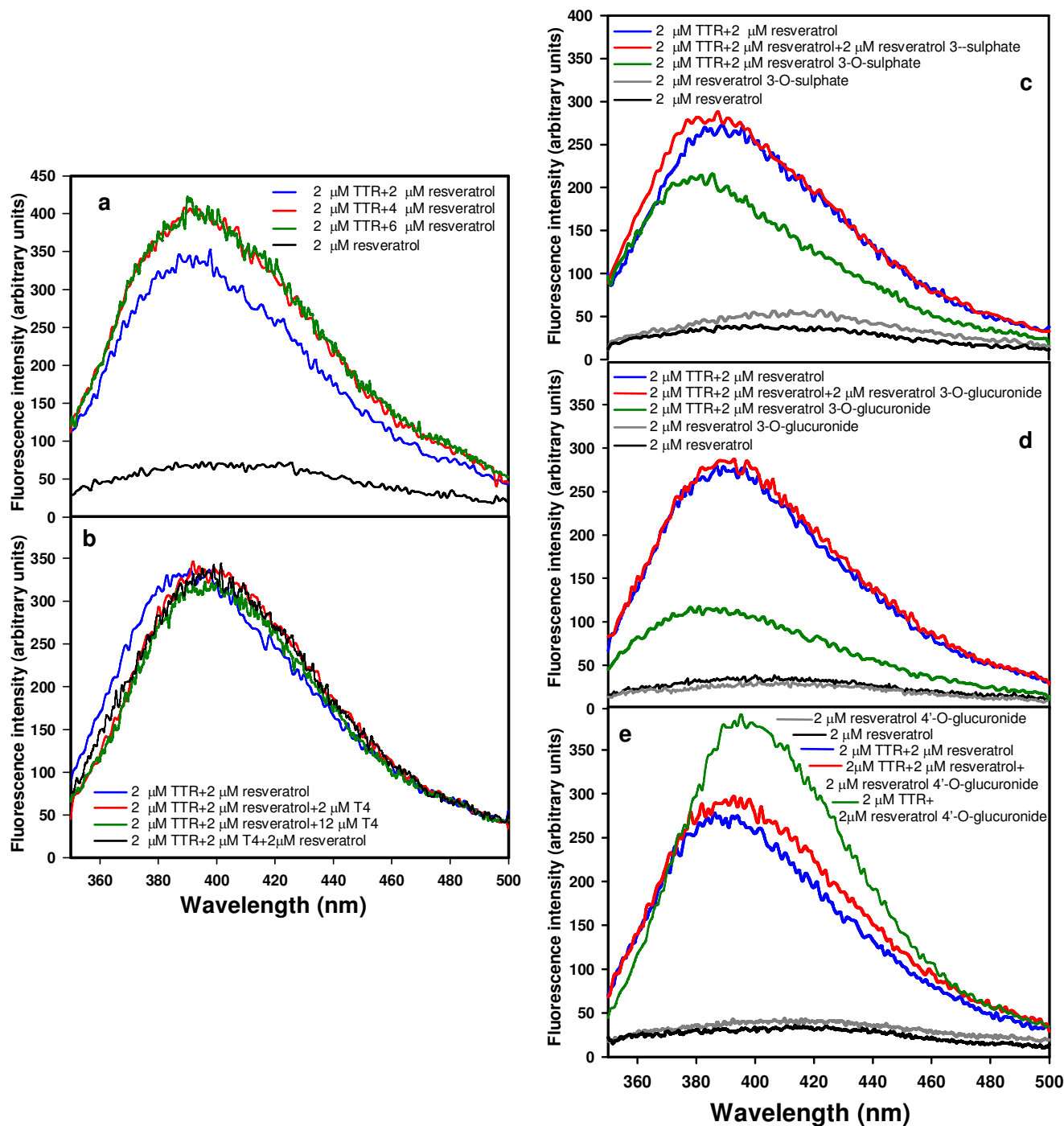
FIGURE 2. **Fluorometric competition assays for the binding of resveratrol, T4, and resveratrol metabolites to WT TTR.** *a*, fluorescence emission spectra (excitation at 320 nm) of 2 μM resveratrol in the absence of TTR (*black*) and of 2 μM (*blue*), 4 μM (*red*), or 6 μM (*green*) resveratrol in the presence of 2 μM WT TTR. *b*, emission spectra (excitation at 320 nm) of 2 μM resveratrol in the presence of 2 μM WT TTR before (*blue*) and after the addition of 2 μM T4 (*red*) or 12 μM T4 (*green*); emission spectra (excitation at 320 nm) of 2 μM resveratrol added to 2 μM WT TTR preincubated with 2 μM T4 (*black*). *c–e*, emission spectra (excitation at 320 nm) of 2 μM uncomplexed resveratrol-3-*O*-sulfate (*c*), resveratrol-3-*O*-glucuronide (*d*), or resveratrol-4'-*O*-glucuronide (*e*) in buffer solution (*gray*) or in the presence of 2 μM WT TTR (*green*). *c–e*, emission spectra of 2 μM uncomplexed resveratrol in buffer solution (*black*) or in the presence of 2 μM WT TTR before (*blue*) and after the addition of 2 μM resveratrol-3-*O*-sulfate (*c*), resveratrol-3-*O*-glucuronide (*d*), or resveratrol-4'-*O*-glucuronide (*e*) (*red*).

sulfate, resveratrol-3-*O*-glucuronide, and resveratrol-4'-*O*-glucuronide) were added to induce the displacement of the radioactive ligand. Indeed, no T4 displacement by resveratrol (Fig. 3*a*) nor by its metabolites (not shown) was observed, at variance with the displacement of radiolabeled T4 by the nonradiolabeled ligand (Fig. 3*b*). The competition experiment was repeated for resveratrol by incubating transthyretin with a mixture of nonradiolabeled T4 (3 μM) and radiolabeled T4 (trace amount); even under these experimental conditions, the resveratrol was not able to displace the bound T4 (Fig. 3*c*), whereas T4 showed the ability to compete for the binding to the protein (Fig. 3*d*), confirming the existence of binding site heterogeneity
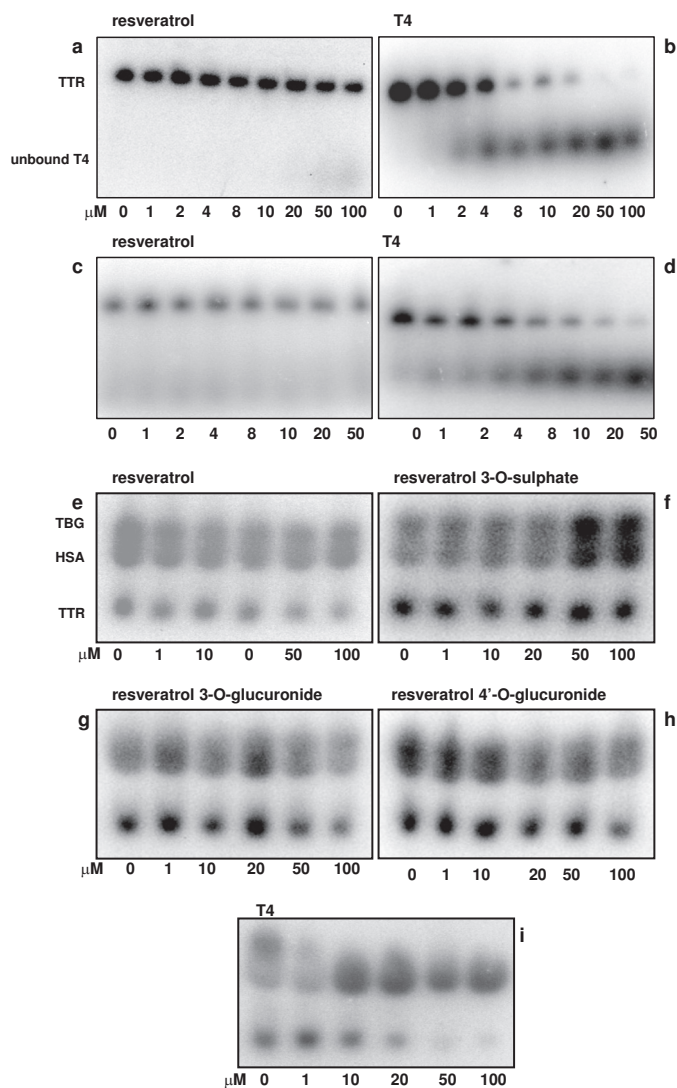
FIGURE 3. **Competition between resveratrol (and its metabolites) and TTR-bound radiolabeled T4 in buffer solution and in human plasma.** Increasing amounts of resveratrol (*a* and *c*) or nonradiolabeled T4 (*b* and *d*) were added in buffer solution to 3 μM WT TTR preincubated with a trace amount of radiolabeled T4 (*a* and *b*) or preincubated with 3 μM nonradiolabeled T4 containing a trace amount of radiolabeled T4 (*c* and *d*). Increasing amounts of resveratrol (*e*), resveratrol-3-*O*-sulfate (*f*), resveratrol-3-*O*-glucuronide (*g*), resveratrol-4′-*O*-glucuronide (*h*), or nonradiolabeled T4 (*i*) were added to human plasma preincubated with a trace amount of radiolabeled T4. Radioactivity signals after nondenaturing PAGE are shown for thyroxine-binding globulin (*TBG*), human serum albumin (*HSA*), and TTR (23).

in TTR. Consistent with the latter results, a limited displacement of TTR-bound radiolabeled T4 in human plasma was found only in the presence of a large excess (50–100 μM) of resveratrol (Fig. 3*e*), whereas essentially no T4 displacement was observed for its metabolites (Fig. 3, *f–h*).

As in the case of resveratrol, the fluorescence emission of resveratrol metabolites is remarkably enhanced upon binding to TTR, and the characteristic emission spectra, distinct for λ_{max} and fluorescence intensity, are obtained for the above mentioned metabolic derivatives bound to TTR (Fig. 2, *c–e*). However, their affinities for TTR were significantly lower than that of resveratrol. In fact, in the presence of equimolar TTR, resveratrol, and its metabolic derivatives, the fluorescence emission spectrum of TTR-bound resveratrol was largely pre-

dominant, indicating at the same time that the binding of resveratrol and its metabolites takes place at the same binding site in the TTR molecule (Fig. 2, *c–e*).

Competition between Resveratrol, Flavonoids, and Their Metabolites and T4—The interactions of some flavonoids and their metabolites with TTR have also been analyzed in competition binding experiments using both resveratrol and radiolabeled T4 as probes. We have found that genistein and apigenin, which are not fluorescent in the emission region of resveratrol, at equimolar concentration relative to resveratrol, were able to nearly completely displace it from TTR, as revealed by the loss of its fluorescence emission intensity (Fig. 4, *a* and *b*). Instead, in the case of daidzein, which exhibits a fluorescence spectrum distinct from that of resveratrol, a binding to TTR weaker than that of resveratrol was observed (Fig. 4*c*). Fluorescence titrations were also carried out to further analyze the competition between resveratrol and flavonoids and their metabolites. In such competitive binding assays, only genistein and apigenin have shown the ability to significantly compete with TTR-bound resveratrol (Fig. 4*d*). In binding experiments using radiolabeled T4 as a probe, a significant T4 displacement was observed only at high genistein concentration (Fig. 5*a*), and the competition by apigenin and daidzein was even weaker (Fig. 5, *b* and *c*, respectively). When the ability of genistein, apigenin, and daidzein to displace TTR-bound radiolabeled T4 in human plasma was investigated to evaluate the binding selectivity of flavonoids for TTR in plasma, genistein (Fig. 5*d*) exhibited the highest binding selectivity, whereas for apigenin (Fig. 5*e*) and daidzein (Fig. 5*f*), rather low binding selectivities were observed. With regard to the flavonoid metabolites genistein-7-*O*-glucuronide and daidzein-7-*O*-glucuronide, they did not significantly compete neither with TTR-bound resveratrol (Fig. 4*d*) nor with radiolabeled T4 bound to both recombinant TTR (not shown) and TTR present in plasma (Fig. 5, *g* and *h*).

Stabilizing Effects against Urea Denaturation and Inhibition of TTR Fibrillogenesis by Polyphenols—When flavonoids, stilbenoids, and their metabolites were tested for their ability to stabilize TTR in the presence of 5 M urea, the relative amount of TTR monomer, as revealed by SDS-PAGE, upon incubation with the denaturing agent followed by protein cross-linking, was assumed to be representative of the fraction of denatured protein present in the sample. The inhibition of TTR fibrillogenesis by polyphenols at moderately acidic pH (pH 4.3) was estimated by monitoring the increase of turbidity of protein solutions, as described under "Experimental Procedures," using diflunisal as a reference fibrillogenesis inhibitor. Stabilizing effects against urea denaturation and inhibition of TTR fibrillogenesis by polyphenols were found to be in fairly good agreement. Significant and similar stabilizing effects against urea denaturation (Fig. 6, *a* and *b*) and inhibition of TTR fibrillogenesis (Fig. 6*c* and 6*d*) were observed for resveratrol and resveratrol-3-*O*-sulfate and for genistein and apigenin, whereas moderate to negligible stabilizing effects against urea denaturation (Fig. 6, *a* and *b*) and inhibitory effects on TTR fibrillogenesis (Fig. 6, *c* and *d*) were found for the other tested polyphenols. In particular, for polyphenols metabolites bearing the glucuronide group, a weak stabilizing effect was observed under the same experimental conditions.
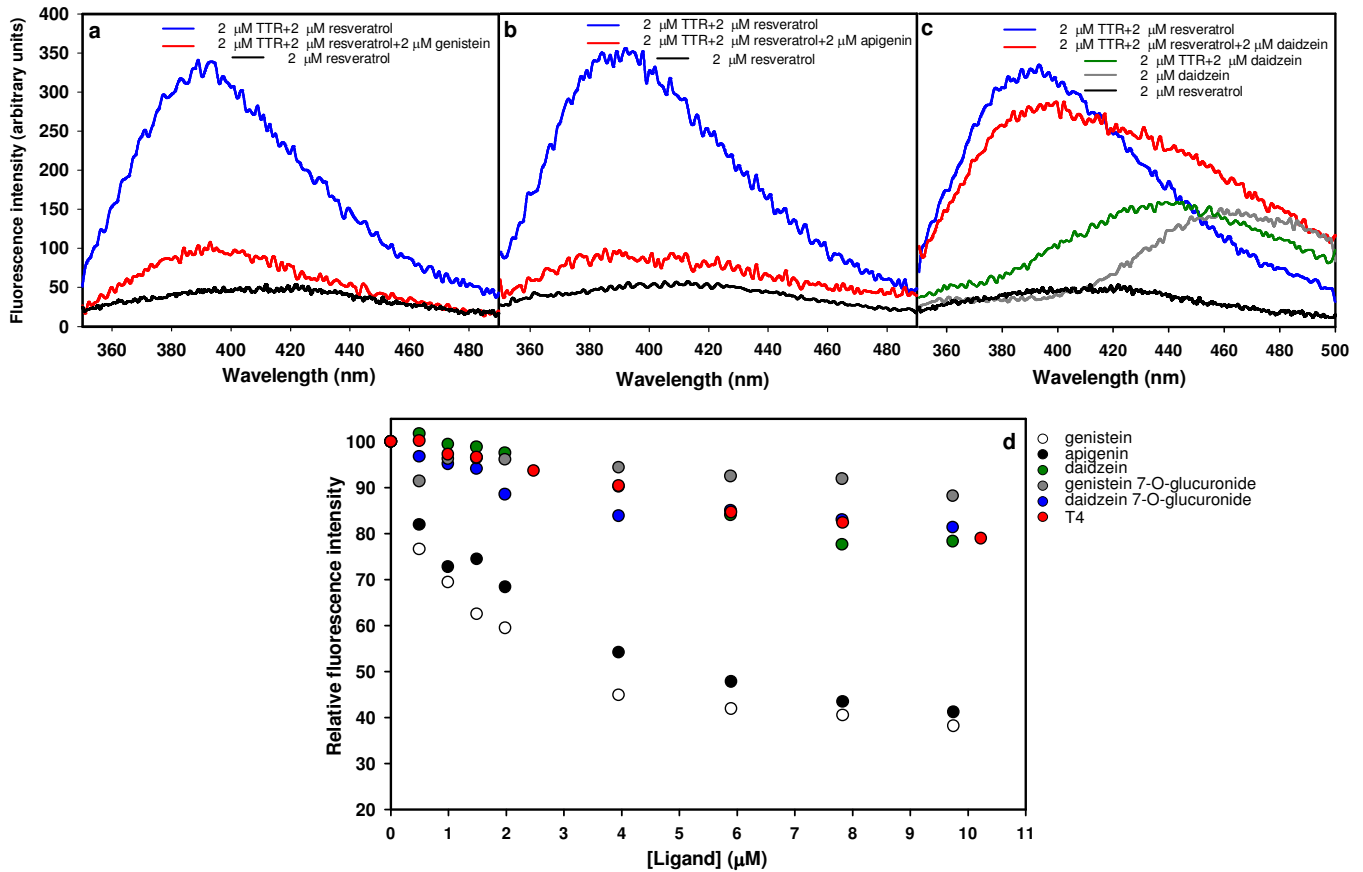
FIGURE 4. **Fluorometric assays for the binding of flavonoids and their metabolites to TTR.** *a–c*, fluorescence emission spectra (excitation at 320 nm) of 2 μM resveratrol in the absence (*black*) or in the presence of 2 μM WT TTR before (*blue*) and after the addition of 2 μM genistein (*a*), apigenin (*b*), or daidzein (*c*) (*red*). *c*, the emission spectra of 2 μM uncomplexed daidzein (*gray*), and in the presence of 2 μM WT TTR (*green*) are also shown. *d*, competitive fluorometric titrations (excitation at 320 nm, and emission at 390 nm) performed by monitoring the displacement of resveratrol (5 μM in the medium) bound to WT TTR (1 μM), in the presence of increasing concentrations of genistein (*white*), apigenin (*black*), daidzein (*green*), genistein-7-O-glucuronide (*gray*), daidzein-7-O-glucuronide (*blue*), or T4 (*red*).
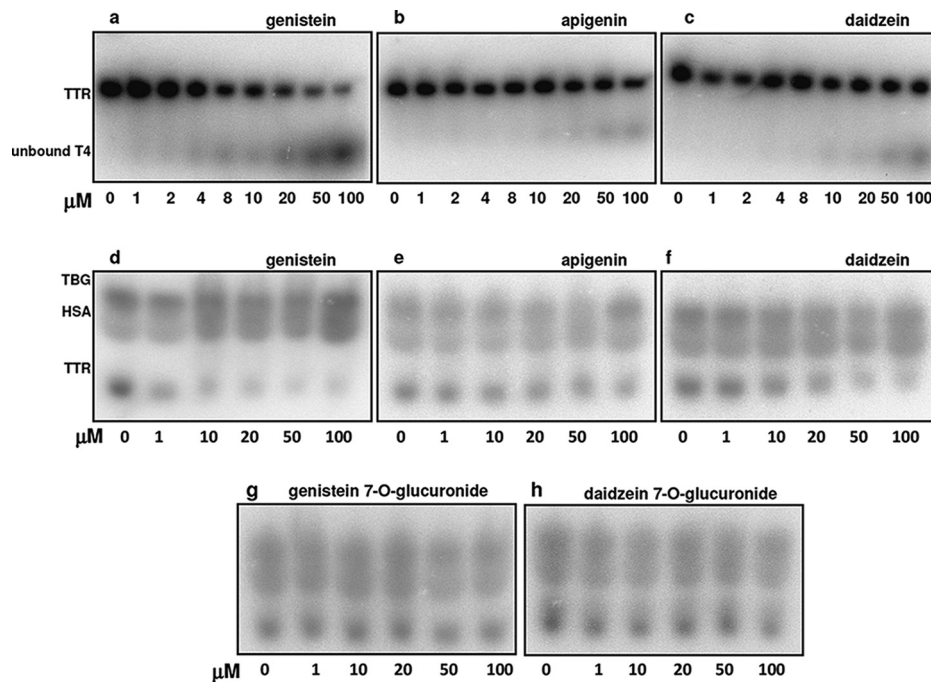

FIGURE 5. **Competition between flavonoids (and their metabolites) and TTR-bound radiolabeled T4 in buffer solution and in human plasma.** *a–c*, increasing amounts of genistein (*a*), apigenin (*b*), and daidzein (*c*) were added in buffer solution to 3 μM WT TTR preincubated with a trace amount of radiolabeled T4. *d–h*, increasing amounts of genistein (*d*), apigenin (*e*), daidzein (*f*), genistein-7-O-glucuronide (*g*), and daidzein-7-O-glucuronide (*h*) were added to human plasma preincubated with a trace amount of radiolabeled T4. Radioactivity signals after nondenaturing PAGE are shown for thyroxine-binding globulin (*TBG*), human serum albumin (*HSA*), and TTR (23).
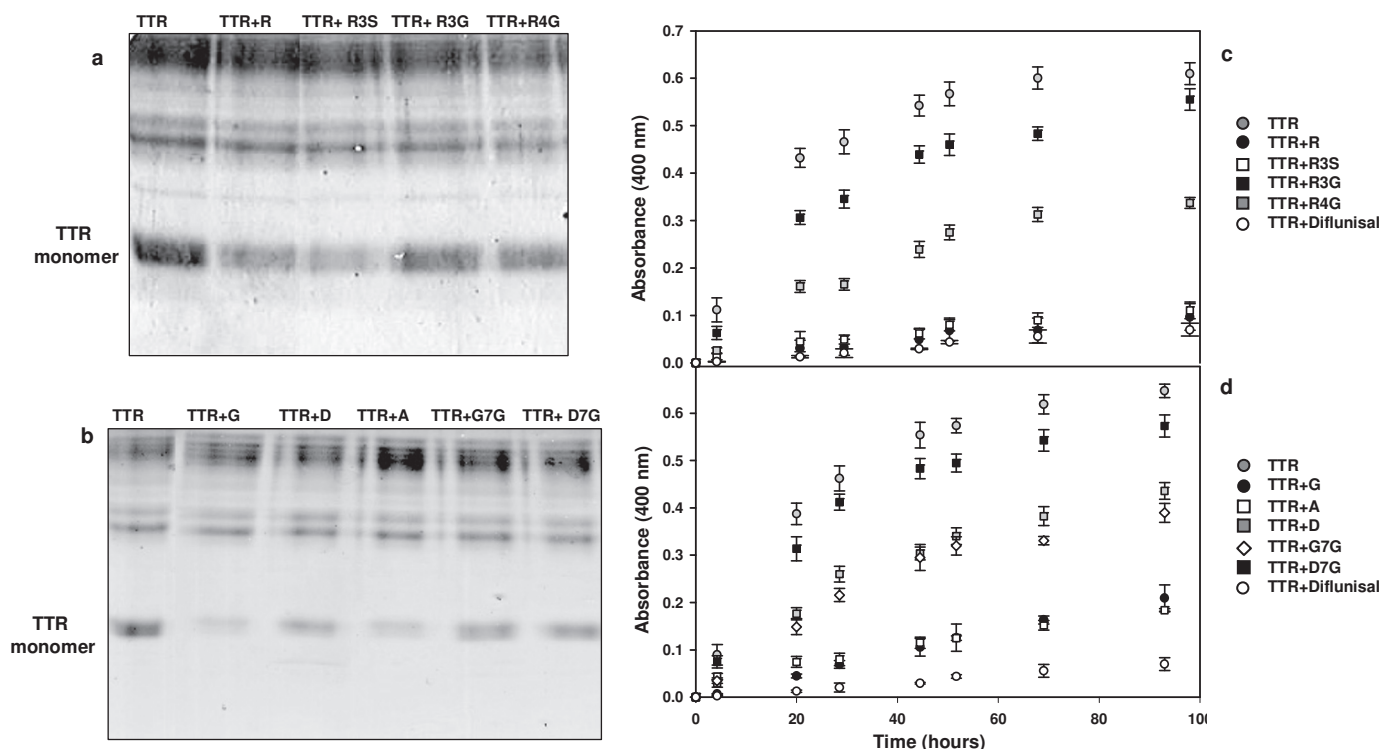
FIGURE 6. **Stabilizing effect on TTR by stilbenoids and flavonoids and stabilization against urea denaturation.** 10 μM WT TTR alone or supplemented with resveratrol and its metabolites (*a*) or with flavonoids and their metabolites (*b*) was incubated in 10 mM sodium phosphate, 150 mM NaCl, pH 7.4, in the presence of 5 M urea for 24 h at 4 °C. Electrophoretic patterns after protein cross-linking with glutaraldehyde and SDS-PAGE are shown. *a*, WT TTR alone (*lane 1*) or supplemented with 20 μM resveratrol (*R, lane 2*), 20 μM resveratrol-3-*O*-sulfate (*R3S, lane 3*), 20 μM resveratrol-3-*O*-glucuronide (*R3G, lane 4*), or 20 μM resveratrol-4'-*O*-glucuronide (*R4G, lane 5*). *b*, WT TTR alone (*lane 1*) or supplemented with 20 μM genistein (*G, lane 2*), 20 μM daidzein (*D, lane 3*), 20 μM apigenin (*A, lane 4*), 20 μM genistein-7-*O*-glucuronide (*G7G, lane 5*), or 20 μM daidzein-7-*O*-glucuronide (*D7G, lane 6*). The experiments shown in *a* and *b* were performed in triplicate, and a representative SDS-PAGE for resveratrol and its metabolites and a representative SDS-PAGE for flavonoids and some of their metabolites are shown. The data (relative amounts of TTR monomers) obtained for TTR alone or in the presence of stilbenoids were: 100% in the absence of ligands, 41.7 $\pm$ 2.6% for resveratrol, 36.2 $\pm$ 3.4% for resveratrol-3-*O*-sulfate, 83 $\pm$ 5.3% for resveratrol-3-*O*-glucuronide, and 69 $\pm$ 3.2% for resveratrol-4'-*O*-glucuronide. The data (relative amounts of TTR monomers) obtained for TTR alone or in the presence of flavonoids were: 100% in the absence of ligands, 36.5 $\pm$ 7.8% for genistein, 40.4 $\pm$ 3.1% for apigenin, 52.1 $\pm$ 3.9% for daidzein, 88.3 $\pm$ 10.2% for genistein-7-*O*-glucuronide, and 83.5 $\pm$ 15.0% for daidzein-7-*O*-glucuronide. Inhibition of TTR fibrillogenesis. *c*, turbidimetric assays for 3.6 μM WT TTR in the absence of ligands (*gray circles*) or preincubated with 3 molar equivalents of resveratrol (*black circles*), resveratrol-3-*O*-sulfate (*white squares*), resveratrol-3-*O*-glucuronide (*black squares*), or resveratrol-4'-*O*-glucuronide (*gray squares*). *d*, turbidimetric assays for 3.6 μM WT TTR in the absence of ligands (*gray circles*) or preincubated with 3 molar equivalents of genistein (black circles), apigenin (*white squares*), daidzein (*gray squares*), genistein-7-*O*-glucuronidated (*white diamonds*), or daidzein-7-*O*-glucuronide (*black squares*). The inhibition of fibrillogenesis by the reference compound diflunisal is also shown (*white circles*) in *c* and *d*. All experiments were performed in triplicate, and the values are reported with *error bars* indicative of standard deviations.

Structure of TTR in Complex with Both Resveratrol and T4— To obtain evidence on a structural basis for the presence of preferential binding sites in TTR, the structure of TTR in complex with stoichiometric amounts of resveratrol and T4 has been determined. The presence of different ligands in the TTR binding sites is not easy to detect even at relatively high resolution, because of the intrinsic disorder introduced in the electron density map by the presence of the 2-fold axis running along the central binding cavity. This can be partially overcome by using T4 as a ligand, because the anomalous signal of iodine atoms allows us to detect unambiguously the presence of the bound hormone. In the case of the mixed complex, resveratrol is clearly visible only at site B (designated B in the crystal, according to Ref. 27) in the electron density map calculated with coefficients $|2F_{\text{obs}} - F_{\text{calc}}|$. Notably, the binding mode of resveratrol is opposite to that described for TTR-bound resveratrol (22), with the 3,5-dihydroxyphenyl moiety now pointing toward the inner part of the cavity, in which hydrogen bond interactions are established with Oγ and the carbonyl group of Ser-117. The same orientation for resveratrol is also observed

for the TTR-resveratrol complex, determined by us in the same experimental conditions at 1.38 Å resolution (data not shown). This different binding mode of resveratrol to TTR observed in crystal structures determined independently in different laboratories is possibly due to the fact that our complexes were prepared in solution and crystallized, whereas the complex in the case of the previous structure (22) was prepared by soaking. A clear density for any ligand is absent at site A (Fig. 7*a*), with the exception of iodine atoms. More specifically, six peaks corresponding to iodine atoms are visible in the anomalous difference Fourier map contoured at 6σ level at site A and only two at site B (Fig. 7*b*). In both sites, the electron density for the light atoms of the hormone are not visible, which suggests that T4 is bound in the TTR cavity in a rather loose way, whereas iodine atoms are detectable because of their high electron content (Fig. 7*a*). Overall, our results indicate that resveratrol is bound essentially at one site (site B), whereas T4 is present mostly in the other site (site A) and only to a minor extent in site B.
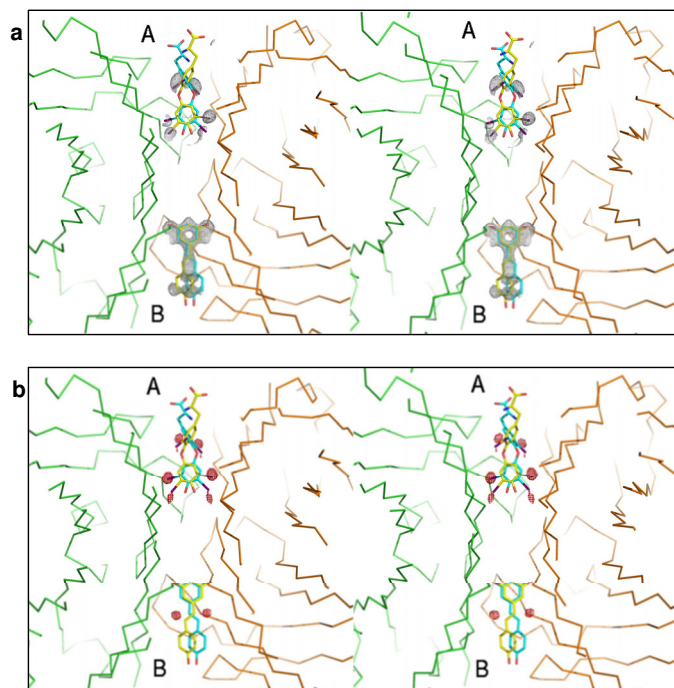
FIGURE 7. **Electron density map of the binding cavities of TTR in complex with both T4 and resveratrol.** ($F_{obs} - F_{calc}$) electron density map (*a*) and anomalous Fourier difference map (*b*) were calculated before fitting any ligand inside the cavities. Phases were calculated from the model. Map (*a*) is contoured at 1.5σ, and map (*b*) is contoured at 5.5σ level. The two ligands, resveratrol and T4, are fitted in site B and A, respectively.

Structures of Complexes of TTR with Polyphenol Metabolites—To gain insight into the molecular basis of the *in vitro* binding properties established for polyphenol metabolites, the structures of WT TTR in complex with some polyphenol metabolites were determined to high resolutions (between 1.25 and 1.50 Å; Table 1). The structures of TTR in complex with resveratrol metabolites are representative of the effect of the presence of the glucuronide group or of the sulfate group bound to the resveratrol molecule.

The binding mode of resveratrol-3-*O*-glucuronide, shown in Fig. 8*a*, resembles that described for TTR-bound resveratrol (22). Accordingly, the 4′-hydroxyl group of the monohydroxyphenyl group is oriented toward the center of the binding site forming hydrogen bonds with the Ser-117 side chain (3.00 Å). The hydroxyphenyl ring bearing at position 3 the glucuronide moiety is oriented toward the solvent, with the Ala-108 side chain fitting in between the two aryl groups, in contact with the ethenyl linker at a distance of 4.02 Å. The glucuronide group is fully displaced outside the cavity, tethering a network of water molecules, together with the Thr-106, Glu-154, and Lys-15 side chains. In the structure of the TTR-resveratrol-4′-*O*-glucuronide complex (Fig. 8*b*), the ligand now exhibits a binding mode similar to that of resveratrol in complex with TTR shown in this work and opposite to that present in the previously published structure of the resveratrol-TTR complex (22). The mode of binding of resveratrol is also opposite to that of the 3-*O*-glucuronide derivative, with the 3,5-dihydroxyphenyl moiety now pointing toward the inner part of the cavity, in which hydrogen bond interactions are established with the Ser-117 side chain and its main chain carbonyl groups (-OH3, O Ser-117 3.51 Å;

-OH3, Oγ Ser-117 2.70 or 2.96 Å; -OH5, O Ser-117′ 3.24 Å; and -OH5, Oγ Ser-117′ 2.80 or 3.16 Å). In this situation, the monohydroxyphenyl ring bearing the glucuronide moiety is oriented toward the solvent. Clearly, the different binding mode of the two TTR-bound glucuronidated derivatives of resveratrol is imposed by the steric hindrance of the glucuronide group, which is fully displaced outside the binding cavity in the case of both glucuronidated derivatives of resveratrol. A binding mode imposed by the presence of the glucuronide moiety outside the binding cavity has also been found for genistein-7-*O*-glucuronide and daidzein-7-*O*-glucuronide (Protein Data Bank codes 5AKV and 5AL8, respectively; Table 1). Overall, the examined glucuronidated polyphenols bind to TTR with their glucuronide moiety sticking of the cavities toward the solvent, because of its steric hindrance. Moreover, the overall polarity of glucuronidated polyphenols is increased, further reducing binding affinity. The poorly defined electron density of the glucuronide moiety is in keeping with the very weak *in vitro* interactions of glucuronidated polyphenols with TTR (Fig. 8).

In the case of TTR in complex with resveratrol-3-*O*-sulfate, the binding mode resembles that described for TTR-bound resveratrol (22) and opposite to that of resveratrol co-crystallized with TTR (this work). The 4′-hydroxyl group of the monohydroxyphenyl group points toward the center of the binding site forming hydrogen bonds with the Ser-117 side chain (-OH4, O Ser-117 2.86 Å). The hydroxyphenyl ring bearing the sulfate group at position 3 is oriented toward the solvent, with such group being positioned between the side chains of Thr-106 and Lys-15′, at 3.06 Å from -OH group of Thr-106 and 2.99 Å from the -NH₂ group of Lys-15′. A torsion angle of 150–160° between the hydroxyphenyl ring bearing the sulfate group and the monohydroxyphenyl ring could be estimated, which is significantly different from that for a fully planar configuration (for a comparison, the torsion angle in the case of TTR-bound resveratrol is close to 180°). Resveratrol-3-*O*-sulphate appears to be a better ligand for TTR compared with glucuronidated polyphenols. This can be attributed to a favorable interaction of the sulfate group with the side chain of Lys-15, as proved by a clear electron density for this group (Fig. 8*c*).

Discussion

A variety of natural polyphenols, such as resveratrol (37), oloeuropein (38), curcumin (29, 39, 40), epigallocatechin-3-gallate (41), and other flavonoids (42), have been reported to inhibit the fibrillogenesis process for amyloid precursor proteins and peptides *in vitro* and possibly *in vivo*. In general, the mechanisms by which these compounds are able to inhibit fibrillogenesis have not been defined. An exception is represented by TTR, for which the inhibition of fibrillogenesis is due to the specific binding of ligands, including polyphenols, to the T4 binding sites, leading to the stabilization of the TTR tetramer (2, 14, 22–26).

In this work, we have compared the ability of resveratrol, flavonoids, and some of their major metabolites to interact with TTR and to stabilize its native state. The results of our binding experiments initially conducted with resveratrol and T4, by using specific and independent signals, strongly indicate that the binding of resveratrol is also characterized by negative

TABLE 1
Data collection and refinement statistics for TTR in complex with ligands

	Resveratrol-3-O-glucuronide	Resveratrol-4′-O-glucuronide	Resveratrol-3-O-sulfate	Genistein-7-O-glucuronide	Daidzein-7-O-glucuronide	Resveratrol-T4
Data collection						
Source	P13 (Petra III, Hamburg, Germany)	P13 (Petra III, Hamburg, Germany)	PXIII (SLS, Villigen, Switzerland)	P13 (Petra III, Hamburg, Germany)	P13 (Petra III, Hamburg, Germany)	PXIII (SLS, Villigen, Switzerland)
Wavelength (Å)	0.967	1.000	1.000	0.967	0.967	1.000
a, b, c (Å)	42.81, 85.27, 63.79	42.74, 85.5, 63.67	42.81 85.56 64.12	42.84, 84.96, 63.64	43.06, 84.88, 63.55	42.54, 85.63, 63.83
Resolution (Å)[a]	63.79–1.25 (1.27–1.25)	63.67–1.35 (1.37–1.35)	42.81–1.39 (1.46–1.39)	63.64–1.52 (1.55–1.52)	84.88–1.50 (1.53–1.50)	42.82–1.54 (1.63–1.54)
R_{merge}[a,b]	0.037 (0.048)	0.031 (0.532)	0.032 (0.371)	0.055 (0.525)	0.051 (0.591)	0.041 (0.298)
R_{pim}[a,c]	0.023 (0.304)	0.020 (0.333)	0.017 (0.275)	0.035 (0.346)	0.032 (0.365)	0.019 (0.143)
$<I/\sigma(I)>$[a]	21.6 (3.5)	26.4 (3.4)	22.8 (3.2)	16.8 (3.0)	17.8 (3.0)	21.3 (4.9)
Completeness (%)[a]	95.1 (80.2)	99.3 (99.1)	96.8 (93.4)	99.9 (98.5)	99.7 (99.6)	99.5 (97.3)
Redundancy[a]	6.7 (6.3)	6.4 (6.6)	3.4 (3.1)	6.5 (6.0)	6.5 (6.7)	6.2 (6.1)
No. reflections[a]	61,920 (2547)	51,577 (2510)	45,697 (5653)	36,372 (1762)	37,976 (1852)	34,821 (4887)
Wilson B-factor	15.5	15.5	14.81	20.09	19.69	17.45
Refinement						
R_{work}/R_{free}[d]	0.17/0.18	0.17/0.19	0.17/0.21	0.17/0.20	0.17/0.19	0.17/0.19
No. atoms	4698	4647	4427	2241	2275	1966
Protein	2144	2143	2384	1952	1980	1793
Ligand	72	68	56	64	62	
Solvent	330	271	264	225	233	173
Average B-factor (Å^2)	22.7	22.2	20.50	27.60	28.60	
Root mean square deviations						
Bond lengths (Å)[e]	0.024	0.011	0.008	0.011	0.012	0.010
Bond angles (°)[e]	2.25	1.52	1.18	1.34	1.38	1.29
Ramachandran plot (%)						
Most favored (%)	92.5	92	92.5	92.0	92.5	91.5
Additionally allowed (%)	7.5	7.5	7.5	8.0	7.5	8.0
Generously allowed (%)	0.0	0.5	0.0	0.0	0.0	0.5
G factor	−0.15	0.04	0.08	0.03	0.04	0.1

[a] The numbers in parentheses refer to the last resolution shell.

[b] $R_{merge} = \Sigma_{hkl}\Sigma_i |I_i(hkl) - <I(hkl)>|/\Sigma_{hkl}\Sigma_i |I_i(hkl)|$.

[c] $R_{pim} = \Sigma_{hkl}(1/N - 1)1/2\Sigma_i |It(hkl) - <I(hkl)>|/\Sigma_{hkl}\Sigma_i|I_i(hkl)|$, where $I(hkl)$ is an individual intensity measurement, and $<I(hkl)>$ is the average intensity for this reflection.

[d] R and $R_{free} = \Sigma hkl||F_o| I |F_c||/\Sigma_{hkl}|F_o|$ for calculating R_{free}, a subset of reflections (5.0%) was randomly chosen as a test set.

[e] The values represent the root mean square deviations from ideal Engh-Huber parameters.
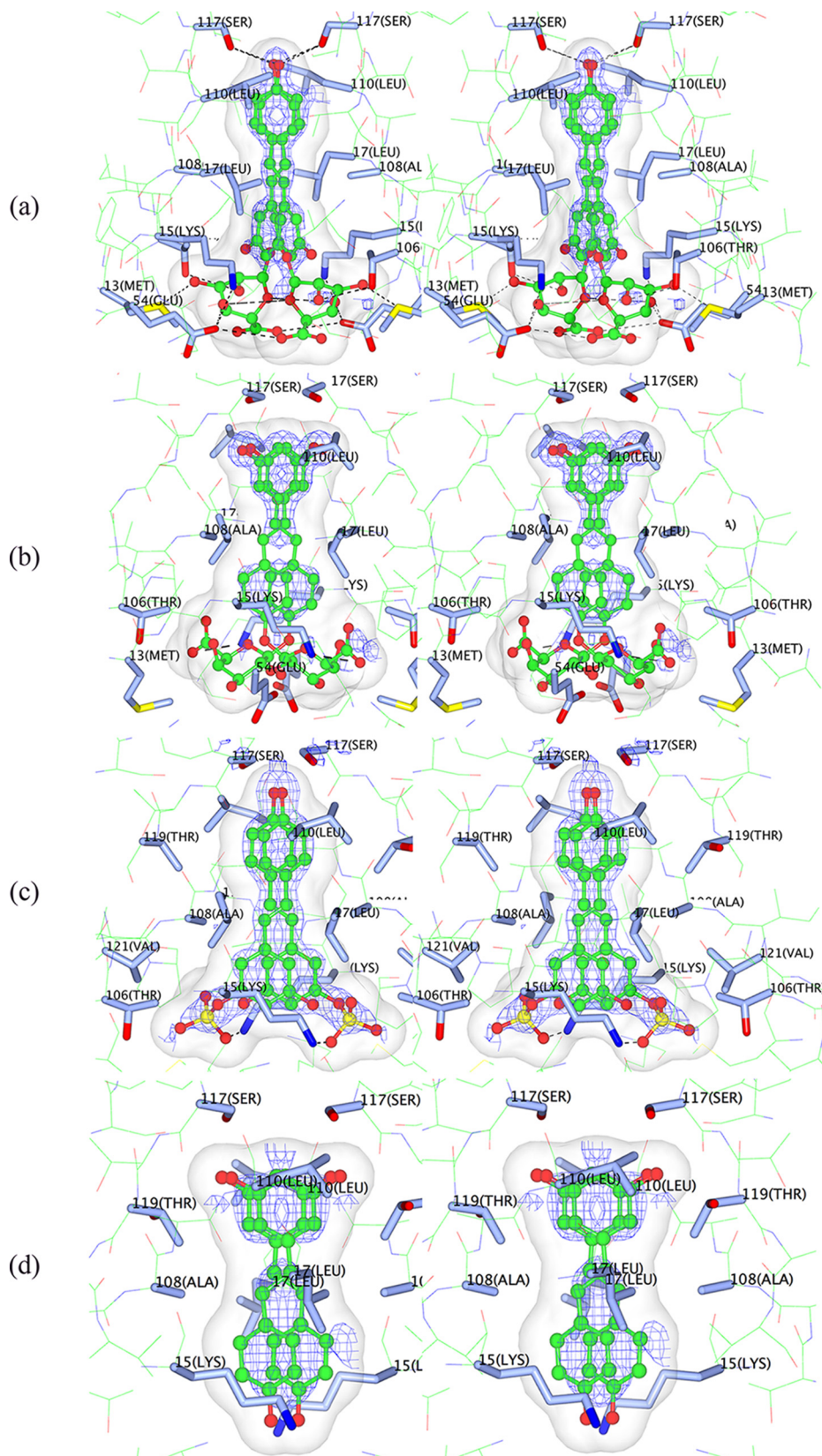
FIGURE 8. **Electron density maps of the binding cavity of TTR in complex with resveratrol metabolites.** *a–c*, electron density maps have been obtained for TTR in complex with resveratrol-3-*O*-glucuronide (*a*), resveratrol-4′-*O*-glucuronide (*b*), and resveratrol-3-*O*-sulfate (*c*). *d*, for a comparison, the structure for resveratrol in complex with one of the two TTR binding sites, as illustrated in Fig. 7, is also shown. Maps were calculated with $|F_{obs} - F_{calc}|$ coefficients, and phases were calculated from the model, deprived of the ligand. Maps are contoured at 3.0σ level. The ligand is shown as a ball and stick model, and the residues of the ligand-binding pocket are shown as thin bonds with atom color coding (carbon, *green*; oxygen, *red*; phosphor, *magenta*; nitrogen, *blue*; sulfur, *yellow*). Side chains in the proximity of the ligand are displayed as *cylinders*. All the ligands are shown with the double orientation generated by the 2-fold symmetry axis.

cooperativity. However, resveratrol exhibits the remarkable feature that its preferential binding site is distinct from that of T4, in such a way that when one of the two ligands is bound to TTR, the other ligand is not able to displace it, in a reciprocal way, even if it is added at high concentration. The presence of binding site heterogeneity in TTR has been confirmed here on a structural basis by the determination of the crystal structure of TTR in complex with both T4 and resveratrol, which has shown that the two ligands bind to distinct preferential binding sites in the crystal. Based on these observations, for a more accurate evaluation of the binding ability of potential candidates as TTR stabilizers, their competition for both T4 and resveratrol preferential binding sites could be analyzed by using the latter ligands as probes.

A feature we have found in our study was the ability of T4 bound at one site of TTR to induce a perturbation (red shift of ∼5 nm) in the emission spectrum of resveratrol bound to the neighbor site of the oligomeric protein. Because the binding of T4 is characterized by a strong negative cooperativity, the hormone is expected to play the role of a negative allosteric effector, able to induce a substantial decrease of the affinity of the second site upon binding to the first high affinity site. However, no evidence has been obtained so far for the communication between subunits mediated by T4 in a protein characterized by a high internal symmetry such as TTR. The spectral perturbation induced by the binding of T4 at one site in the neighbor site occupied by resveratrol may indeed represent the first evidence for an intersubunit communication associated with the modulation of binding affinity in this oligomeric protein.

All the compounds examined in this study proved to be able to interact with TTR, on the basis of direct and competition binding assays and of structural analyses. In particular, among the examined compounds the strongest interaction was found for genistein, which was able to effectively compete with TTR-bound resveratrol and to a lower extent even with TTR-bound T4. Overall, the examined polyphenols (aglycons) possess much higher binding affinities for the preferential resveratrol-binding site in comparison with the preferential binding site of T4.

The rapid and efficient metabolism of polyphenols raises the question as to whether polyphenol metabolites are still endowed with anti-amyloidogenic activity. The results of our investigation confirm that for the analysis of the anti-amiloydogenic potential of natural polyphenols, the effectiveness of their metabolites as fibrillogenesis inhibitors should primarily be evaluated. In this respect, in general the rapid metabolism of polyphenols abrogates substantially their anti-amyloidogenic potential. In particular, we have established that binding affinities and capacities to stabilize TTR are markedly weak for the glucuronidated derivatives of polyphenols in comparison with their aglycons, probably because of the steric hindrance of the glucuronide moiety, as revealed by x-ray analyses, which impedes to a large portion of such polyphenols to fit inside the T4 binding cavities. An exception is represented by the metabolite resveratrol-3-*O*-sulfate, which exhibits significant stabilizing properties on the TTR molecule, because of a specific interaction of the sulfate group with the Lys-15 side chain, near the entrance of TTR binding sites.

References

1. Westermark, P., Sletten, K., Johansson, B., and Cornwell, G. G., 3rd (1990) Fibril in senile systemic amyloidosis is derived from normal transthyretin. *Proc. Natl. Acad. Sci. U.S.A.* **87,** 2843–2845

2. Johnson, S. M., Wiseman, R. L., Sekijima, Y., Green, N. S., Adamski-Werner, S. L., and Kelly, J. W. (2005) Native state kinetic stabilization as a strategy to ameliorate protein misfolding diseases: A focus on the transthyretin amyloidoses. *Acc. Chem. Res.* **38,** 911–921

3. Benson, M. D., and Kincaid, J. C. (2007) The molecular biology and clinical features of amyloid neuropathy. *Muscle Nerve* **36,** 411–423

4. Monaco, H. L., Rizzi, M., and Coda, A. (1995) Structure of a complex of 2 plasma-proteins: transthyretin and retinol-binding protein. *Science* **268,** 1039–1041

5. Wojtczak, A., Cody, V., Luft, J. R., and Pangborn, W. (1996) Structures of human transthyretin complexed with thyroxine at 2.0 angstrom resolution and 3′,5′-dinitro-N-acetyl-L-thyronine at 2.2 angstrom resolution. *Acta Crystallogr. D* **52,** 758–765

6. Ferguson, R. N., Edelhoch, H., Saroff, H. A., Robbins, J., and Cahnmann, H. J. (1975) Negative cooperativity in the binding of thyroxine to human serum prealbumin. Preparation of tritium-labeled 8-anilino-1-naphthalenesulfonic acid. *Biochemistry* **14,** 282–289

7. Cendron, L., Trovato, A., Seno, F., Folli, C., Alfieri, B., Zanotti, G., and Berni, R. (2009) Amyloidogenic potential of transthyretin variants: insights from structural and computational analyses. *J. Biol. Chem.* **284,** 25832–25841

8. McCutchen, S. L., Colon, W., and Kelly, J. W. (1993) Transthyretin mutation Leu-55-Pro significantly alters tetramer stability and increases amyloidogenicity. *Biochemistry* **32,** 12119–12127

9. McCutchen, S. L., Lai, Z., Miroy, G. J., Kelly, J. W., and Colón, W. (1995) Comparison of lethal and nonlethal transthyretin variants and their relationship to amyloid disease. *Biochemistry* **34,** 13527–13536

10. Shnyrov, V. L., Villar, E., Zhadan, G. G., Sanchez-Ruiz, J. M., Quintas, A., Saraiva, M. J., and Brito, R. M. (2000) Comparative calorimetric study of non-amyloidogenic and amyloidogenic variants of the homotetrameric protein transthyretin. *Biophys. Chem.* **88,** 61–67

11. Hammarström, P., Sekijima, Y., White, J. T., Wiseman, R. L., Lim, A., Costello, C. E., Altland, K., Garzuly, F., Budka, H., and Kelly, J. W. (2003) D18G transthyretin is monomeric, aggregation prone, and not detectable in plasma and cerebrospinal fluid: A prescription for central nervous system amyloidosis? *Biochemistry* **42,** 6656–6663

12. Ferrão-Gonzales, A. D., Palmieri, L., Valory, M., Silva, J. L., Lashuel, H., Kelly, J. W., and Foguel, D. (2003) Hydration and packing are crucial to amyloidogenesis as revealed by pressure studies on transthyretin variants that either protect or worsen amyloid disease. *J. Mol. Biol.* **328,** 963–974

13. Hurshman Babbes, A. R., Powers, E. T., and Kelly, J. W. (2008) Quantification of the thermodynamically linked quaternary and tertiary structural stabilities of transthyretin and its disease-associated variants: The relationship between stability and amyloidosis. *Biochemistry* **47,** 6969–6984

14. Connelly, S., Choi, S., Johnson, S. M., Kelly, J. W., and Wilson, I. A. (2010) Structure-based design of kinetic stabilizers that ameliorate the transthy-

retin amyloidoses. *Curr. Opin. Struct. Biol.* **20,** 54–62

15. Kolstoe, S. E., Mangione, P. P., Bellotti, V., Taylor, G. W., Tennent, G. A., Deroo, S., Morrison, A. J., Cobb, A. J., Coyne, A., McCammon, M. G., Warner, T. D., Mitchell, J., Gill, R., Smith, M. D., Ley, S. V., Robinson, C. V., Wood, S. P., and Pepys, M. B. (2010) Trapping of palindromic ligands within native transthyretin prevents amyloid formation. *Proc. Natl. Acad. Sci. U.S.A.* **107,** 20483–20488

16. Zanotti, G., Cendron, L., Folli, C., Florio, P., Imbimbo, B. P., and Berni, R. (2013) Structural evidence for native state stabilization of a conformationally labile amyloidogenic transthyretin variant by fibrillogenesis inhibitors. *FEBS Lett.* **587,** 2325–2331

17. Coelho, T., Maia, L. F., da Silva, A. M., Cruz, M. W., Planté-Bordeneuve, V., Suhr, O. B., Conceiçao, I., Schmidt, H. H., Trigo, P., Kelly, J. W., Labaudinière, R., Chan, J., Packman, J., and Grogan, D. R. (2013) Long-term effects of tafamidis for the treatment of transthyretin familial amyloid polyneuropathy. *J. Neurol.* **260,** 2802–2814

18. Berk, J. L., Suhr, O. B., Obici, L., Sekijima, Y., Zeldenrust, S. R., Yamashita, T., Heneghan, M. A., Gorevic, P. D., Litchy, W. J., Wiesman, J. F., Nordh, E., Corato, M., Lozza, A., Cortese, A., Robinson-Papp, J., Colton, T., Rybin, D. V., Bisbee, A. B., Ando, Y., Ikeda, S., Seldin, D. C., Merlini, G., Skinner, M., Kelly, J. W., Dyck, P. J., and Diflunisal Trial Consortium (2013) Repurposing diflunisal for familial amyloid polyneuropathy. A randomized clinical trial. *JAMA* **310,** 2658–2667

19. Obici, L., and Merlini, G. (2014) An overview of drugs currently under investigation for the treatment of transthyretin-related hereditary amyloidosis. *Expert Opin. Investig. Drugs* **23,** 1239–1251

20. Del Rio, D., Rodriguez-Mateos, A., Spencer, J. P., Tognolini, M., Borges, G., and Crozier, A. (2013) Dietary (poly)phenolics in human health: structures, bioavailability, and evidence of protective effects against chronic diseases. *Antioxid. Redox Signal.* **18,** 1818–1892

21. Bieschke, J. (2013) Natural compounds may open new routes to treatment of amyloid diseases. *Neurotherapeutics* **10,** 429–439

22. Klabunde, T., Petrassi, H. M., Oza, V. B., Raman, P., Kelly, J. W., and Sacchettini, J. C. (2000) Rational design of potent human transthyretin amyloid disease inhibitors. *Nat. Struct. Biol.* **7,** 312–321

23. Radović, B., Mentrup, B., and Köhrle, J. (2006) Genistein and other soya isoflavones are potent ligands for transthyretin in serum and cerebrospinal fluid. *Brit. J. Nutr.* **95,** 1171–1176

24. Trivella, D. B., dos Reis, C. V., Lima, L. M., Foguel, D., and Polikarpov, I. (2012) Flavonoid interactions with human transthyretin: combined structural and thermodynamic analysis. *J. Struct. Biol.* **180,** 143–153

25. Trivella, D. B., Bleicher, L., Palmieri, L. D., Wiggers, H. J., Montanari, C. A., Kelly, J. W., Lima, L. M., Foguel, D., and Polikarpov, I. (2010) Conformational differences between the wild type and V30M mutant transthyretin modulate its binding to genistein: implications to tetramer stability and ligand-binding. *J. Struct. Biol.* **170,** 522–531

26. Green, N. S., Foss, T. R., and Kelly, J. W. (2005) Genistein, a natural product from soy, is a potent inhibitor of transthyretin amyloidosis. *Proc. Natl. Acad. Sci. U.S.A.* **102,** 14545–14550

27. Cianci, M., Folli, C., Zonta, F., Florio, P., Berni, R., and Zanotti, G. (2015) Structural evidence for asymmetric ligand binding to transthyretin. *Acta Crystallogr. D* **71,** 1582–1592

28. Pasquato, N., Berni, R., Folli, C., Alfieri, B., Cendron, L., and Zanotti, G. (2007) Acidic pH-induced conformational changes in amyloidogenic mutant transthyretin. *J. Mol. Biol.* **366,** 711–719

29. Pullakhandam, R., Srinivas, P. N., Nair, M. K., and Reddy, G. B. (2009) Binding and stabilization of transthyretin by curcumin. *Arch. Biochem. Biophys.* **485,** 115–119

30. Miller, S. R., Sekijima, Y., and Kelly, J. W. (2004) Native state stabilization by NSAIDs inhibits transthyretin amyloidogenesis from the most common familial disease variants. *Lab. Invest.* **84,** 545–552

31. Kabsch, W. (2010) Integration, scaling, space-group assignment and postrefinement. *Acta Crystallogr. D* **66,** 133–144

32. Evans, P. (2006) Scaling and assessment of data quality. *Acta Crystallogr. D* **62,** 72–82

33. Hörnberg, A., Eneqvist, T., Olofsson, A., Lundgren, E., and Sauer-Eriksson, A. E. (2000) A comparative analysis of 23 structures of the amyloidogenic protein transthyretin. *J. Mol. Biol.* **302,** 649–669

34. Adams, P. D., Afonine, P. V., Bunkóczi, G., Chen, V. B., Davis, I. W., Echols, N., Headd, J. J., Hung, L. W., Kapral, G. J., Grosse-Kunstleve, R. W., McCoy, A. J., Moriarty, N. W., Oeffner, R., Read, R. J., Richardson, D. C., Richardson, J. S., Terwilliger, T. C., and Zwart, P. H. (2010) PHENIX: a comprehensive Python-based system for macromolecular structure solution. *Acta Crystallogr. D* **66,** 213–221

35. Emsley, P., Lohkamp, B., Scott, W. G., and Cowtan, K. (2010) Features and development of Coot. *Acta Crystallogr. D* **66,** 486–501

36. Schüttelkopf, A. W., and van Aalten, D. M. (2004) PRODRG: a tool for high-throughput crystallography of protein-ligand complexes. *Acta Crystallogr. D* **60,** 1355–1363

37. Ge, J. F., Qiao, J. P., Qi, C. C., Wang, C. W., and Zhou, J. N. (2012) The binding of resveratrol to monomer and fibril amyloid beta. *Neurochem. Int.* **61,** 1192–1201

38. Rigacci, S., Guidotti, V., Bucciantini, M., Nichino, D., Relini, A., Berti, A., and Stefani, M. (2011) A beta (1–42) Aggregates into non-toxic amyloid assemblies in the presence of the natural polyphenol oleuropein aglycon. *Curr. Alzheimer Res.* **8,** 841–852

39. Daval, M., Bedrood, S., Gurlo, T., Huang, C. J., Costes, S., Butler, P. C., and Langen, R. (2010) The effect of curcumin on human islet amyloid polypeptide misfolding and toxicity. *Amyloid* **17,** 118–128

40. Yang, F., Lim, G. P., Begum, A. N., Ubeda, O. J., Simmons, M. R., Ambegaokar, S. S., Chen, P. P., Kayed, R., Glabe, C. G., Frautschy, S. A., and Cole, G. M. (2005) Curcumin inhibits formation of amyloid beta oligomers and fibrils, binds plaques, and reduces amyloid *in vivo. J. Biol. Chem.* **280,** 5892–5901

41. Bieschke, J., Russ, J., Friedrich, R. P., Ehrnhoefer, D. E., Wobst, H., Neugebauer, K., and Wanker, E. E. (2010) EGCG remodels mature alpha-synuclein and amyloid-beta fibrils and reduces cellular toxicity. *Proc. Natl. Acad. Sci. U.S.A.* **107,** 7710–7715

42. Hirohata, M., Ono, K., Takasaki, J., Takahashi, R., Ikeda, T., Morinaga, A., and Yamada, M. (2012) Anti-amyloidogenic effects of soybean isoflavones in vitro: fluorescence spectroscopy demonstrating direct binding to A beta monomers, oligomers and fibrils. *Biochim. Biophys. Acta* **1822,** 1316–1324